PHYSICAL REVIEW E **78**, 030701(R) (2008)

Elasticity-mediated nematiclike bacterial organization in model extracellular DNA matrix

Ivan I. Smalyukh,[1,2,*] John Butler,[1] Joshua D. Shrout,[3,4] Matthew R. Parsek,[4] and Gerard C. L. Wong[1,5,†]
[1]*Department of Materials Science and Engineering, University of Illinois at Urbana-Champaign, Urbana, Illinois 61801, USA*
[2]*Department of Physics and the Liquid Crystal Materials Research Center, University of Colorado at Boulder, Boulder, Colorado 80309, USA*
[3]*Department of Microbiology, University of Washington, P.O. Box 357242, Seattle, Washington 98195, USA*
[4]*Department of Civil Engineering and Geological Sciences, University of Notre Dame, Notre Dame, Indiana 46556, USA*
[5]*Department of Physics, University of Illinois at Urbana-Champaign, Urbana, Illinois 61801, USA*
(Received 14 June 2008; published 23 September 2008)

DNA is a common extracellular matrix component of bacterial biofilms. We find that bacteria can spontaneously order in a matrix of aligned concentrated DNA, in which rod-shaped cells of *Pseudomonas aeruginosa* follow the orientation of extended DNA chains. The alignment of bacteria is ensured by elasticity and liquid crystalline properties of the DNA matrix. These findings show how behavior of planktonic bacteria may be modified in extracellular polymeric substances of biofilms and illustrate the potential of using complex fluids to manipulate embedded nanosized and microsized active particles.

DOI: 10.1103/PhysRevE.78.030701 PACS number(s): 61.30.−v, 82.70.−y, 61.25.H−, 77.84.Nh

Most bacteria live in surface-associated multicellular communities known as biofilms. Unlike their free-floating planktonic counterparts, bacteria in biofilms are encapsulated in a protective matrix of extracellular polymeric substances (EPS) and are strongly resistant to antibiotics [1,2]. Although biofilms are responsible for many problems in industry and agriculture as well as for lethal infections, they can also perform useful functions, such as hydrocarbon breakdown in oil spills and waste water treatment. The EPS matrix of naturally occurring bacterial biofilms is a complex mixture of macromolecules including proteins, exopolysaccharides, and DNA [2,3], the last of which has recently been shown to be an important functional component of biofilm structure [3]. Addition of DNase I to the culture medium strongly inhibits or prevents biofilm formation (although it does not alter growth of individual cells) and can result in "dissolution" of well-established biofilms [3,4]. Bacterial biofilms grow in the airways of Cystic Fibrosis (CF) patients, where DNA concentration can reach 20 mg/ml [5]. Detailed knowledge of the interaction mechanisms of bacteria with semiflexible polymers such as DNA is essential for understanding bacterial biofilms in these environments [2].

The ability to manipulate bacterial genomes has revolutionized our understanding of bacteria [2]. Recently, physical methods such as nanofabrication, microcontact printing, and microfluidics have been used to gain insight into bacterial behavior [6–10]. Much less work, however, has been done from the perspective of bacteria as an active colloidal complex fluid, where individual cells exhibit hierarchical interactions with each other and with their environment. Indeed, inert colloidal objects embedded in complex fluids [11–14] as well as water suspensions of self-propelled particles such as bacteria [15] exhibit a rich diversity of interactions. However, it is not known how different components of the EPS matrix affect bacterial organization. In this Rapid Communication, we demonstrate that *Pseudomonas aeruginosa* can self-organize into a nematiclike ordered state via elastic interactions with an extracellular matrix of DNA. This is unexpected since most bacteria (including *P. aeruginosa*) do not form ordered structures by themselves, despite their elongated shapes [15–17]. We find that the interaction between bacteria and the elastic matrix of concentrated DNA influences the average orientation and motility of *P. aeruginosa*. In such a DNA matrix, rod-shaped bacteria follow the extended DNA chains and the liquid crystalline (LC) director $\hat{n}$ describing their local average orientation (Fig. 1); we show why this is the case. These results demonstrate a simple approach to organize active matter in the nanoscopic and microscopic regimes. Cell alignment can be also important from the biological perspective, since it can impinge on bacterial signaling and differentiation [18,19].

We used a Nikon E200POL polarizing and a Leica TCS SP2 confocal microscopes with fluorescence attachments. Images were acquired using a 63× oil-immersion objective with numerical aperture of 1.4. The studies where performed using λ-phage DNA molecules (New England BioLabs, Inc.) that contain 48 502 base pairs and have ≈16.3 μm contour length and ≈50 nm persistence length. DNA molecules were

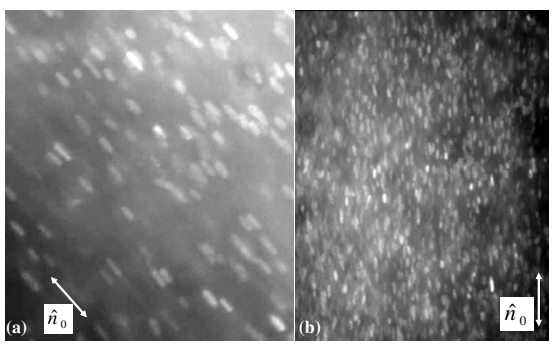

FIG. 1. Fluorescence images of unidirectionally aligned *P. aeruginosa* cells in the aligned LC matrix of concentrated DNA; the number density of bacteria increases from (a) to (b). The signal is from the green fluorescent protein in cells.

*ivan.smalyukh@colorado.edu
†gclwong@illinois.edu

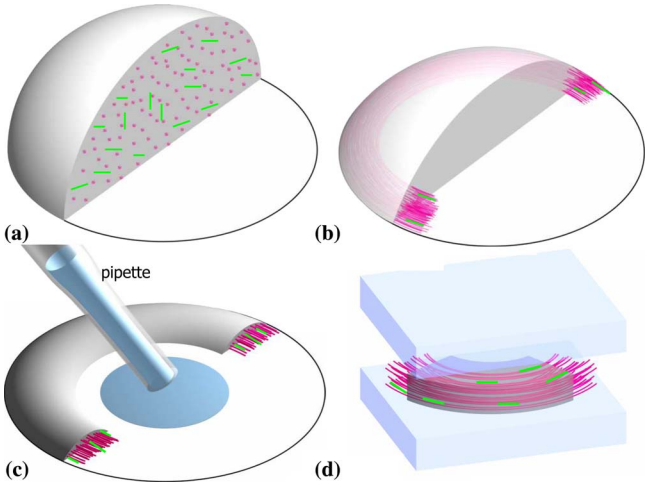

FIG. 2. (Color online) Schematics of the sample preparation procedure. (a) A droplet containing aqueous DNA in the globular states (red) and the rod-shaped bacteria (green) is placed on a clean glass plate. (b) Biopolymers and bacteria are concentrated in a narrow ring next to the contact line; DNA biopolymers are stretched in directions parallel to the contact line and the rod-shaped cells follow their orientations. (c) Residual water from the droplet's center is removed using a microsyringe. (d) Aqueous DNA with concentric LC director and bacteria orientations, obtained after the sample is covered by a glass plate to prevent further water evaporation.

ethanol-precipitated and then resuspended in deionized millipore water at desired concentration. The initial concentration of semidilute aqueous DNA was within $C_{\mathrm{DNA}}=(0.1-2)$ mg/ml. We used *P. aeruginosa* cells inoculated from frozen stock and grown in the Lysogeny broth in a shaker overnight; optical density of cells in the broth was within the range $\rho_{\mathrm{OD}}=0.5-1$.

There are two types of bacterial appendages for motility in the context of *P. aeruginosa* biofilm formation, flagella and type IV pili. The flagellum is well known for being responsible for swimming and swarming motility [20], while type IV pili are involved in twitching motility [21], in which movement occurs via pilus extension and retraction. In addition to the wild-type *P. aeruginosa* cells, we used two mutant strains defective in two types of motility: A flagellum-deficient *fliC* mutant [22] (the *fliC* gene encoding flagellin, the structural subunit of the flagellum), and a type IV pili deficient *pilA* mutant (the pilA gene encodes for a component of pilin, a structural subunit of type IV pili) [20]. *P. aeruginosa* cells have typical radii within $R=(250-400)$ nm and length $L=(1.8-3)$ μm [2,23]. In order to minimize the effects of adventitious genetic mutations, cells from a frozen stock of a single colony were used for all experiments. Before each experiment, we adjusted the density of bacteria to obtain $\rho_{\mathrm{OD}}=0.01-0.1$. We then thoroughly mixed this suspension with a semidilute solution of aqueous DNA at $C_{\mathrm{DNA}}=(0.1-2)$ mg/ml in the proportion 1:1.

The *P. aeruginosa* strains contained a chromosomal, constitutive, green fluorescent protein (GFP)-producing insertion that allows selective visualization of live cells using fluorescence microscopy. A small quantity (~0.01 wt. %) of propidium iodide was added to the growth medium in order to visualize the dead cells. This dye penetrates through the disrupted membrane of a dead cell and intercalates between the base pairs of DNA, which results in ~30-fold enhancement of the fluorescence signal and allows for visualization of the dead cells. The absorption maximum for this dye (when bound to the DNA) is at 535 nm and the fluorescence emission maximum is at 617 nm, which allows its fluorescence signal to be separated from that of GFP of living cells using optical filters. In some of the samples, small quantities of DNA were fluorescently labeled with YOYO-1 dye (molecular probes, one YOYO-1 molecule per 15 bp of DNA) and then added to the unlabeled DNA in proportion ~1:1 000 000; this allowed us to probe the conformation states and orientations of DNA molecules [24].

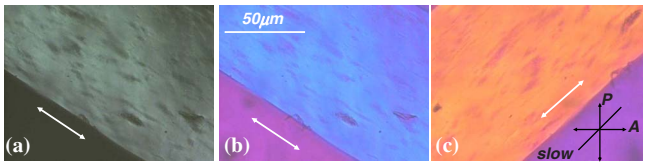

FIG. 3. (Color online) Polarizing microscopy textures of the LC film formed by DNA biopolymers obtained (a) between crossed polarizers, and (b) and (c) with additional retardation plate inserted into the optical path; the orientations of polarizers and "slow" axis of the plate are shown in (c). $\hat{n}_0$ is marked by the white double arrow. The second-order blue and first-order yellow interference colors in (b) and (c) indicate addition and/or subtraction of the optical phase shift when the inserted retardation plate has the "slow" axis perpendicular and/or parallel to $\hat{n}_0$ in the DNA LC with negative optical anisotropy.

Aligned and extended DNA chains are prepared at the contact line of a droplet of aqueous DNA solution, using a modified version of the "coffee ring" method [24]. Droplets of the aqueous DNA-bacteria system of initial volume $(1-50)$ μl were placed on a clean glass plate using a micropipette [Fig. 2(a)]. Since the contact line of the droplet is pinned, the evaporation flux is the strongest next to drop's edge and causes flow from the interior toward periphery, as needed to compensate for the evaporation losses [25]. Using fluorescence microscopy, we observe that this radial outward flow transports both DNA and bacteria to the drop's perimeter [Fig. 2(b)]. DNA chains are stretched to nearly entire contour length and aligned parallel to the pinned contact line, forming a birefringent LC ring at drop's perimeter [Fig. 2(b)]. When most of the DNA biopolymers and bacteria are concentrated at the drop's periphery, we use a microsyringe to remove the residual water from the central part of the droplet. This leaves a concentrated ring of viscous aqueous DNA solution (estimated concentration is $\geqslant$50 mg/ml) with living bacteria [Fig. 2(c)]. We then cover the preparation with a thin cover slide in order to prevent further water evaporation [Fig. 2(d)]. Using a 530 nm retardation plate inserted between microscope's crossed polarizers and a Michel-Levy interference color chart, we determine the director orientation marked by white arrows in Fig. 3. The birefringent LC films between two glass plates have concentric alignment of DNA biopolymers, thickness $(5-50)$ μm, and width of several hundred microns (Fig. 3). The GFP-tagged bacteria are found to follow the orientation of the

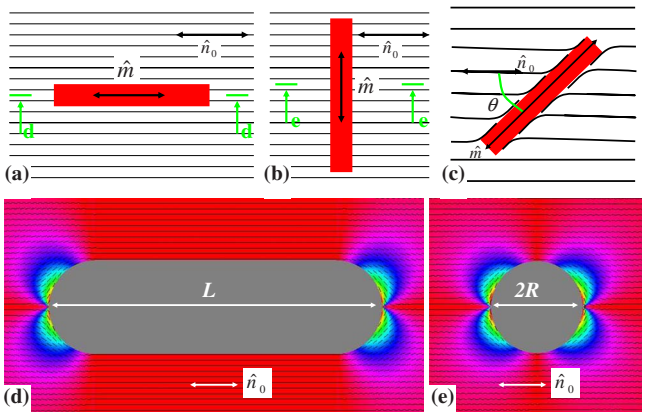

FIG. 4. (Color online) Rods in the ordered biopolymer matrix. Schematics of a rod oriented (a) parallel, (b) perpendicular, and (c) at an angle θ with respect to the far-field LC director $\hat{n}_0$. (d), (e) Computer-simulated alignment of the director $\hat{n}$ (and DNA molecules) around a rod-shaped object (d) parallel and (e) perpendicular to $\hat{n}_0$ in the cross sections marked in (a) and (b).

stretched DNA molecules and the director $\hat{n}$ (Fig. 1). Furthermore, the bacteria are viable, as indicated by monitoring fluorescence from both GFP and propidium iodide.

To characterize the alignment properties of the bacteria in the DNA matrix, we have estimated the order parameter $[s=(3\langle\cos^2\theta\rangle-1)/2$ [26], where θ is the angle between the rod-shaped cell and the local $\hat{n}]$ using the fluorescence images. Surprisingly, we have values $s=0.7-0.9$ that vary depending on sample preparation (DNA concentration, substrate properties, droplet's volume); for comparison, $s=0.3-0.7$ for thermotropic nematics. With no DNA, we observe no ordering of *P. aeruginosa* as we continue to increase their concentration in a drying droplet until the tight packing is achieved, which indicates that DNA plays a critical role in the mechanism of bacterial alignment.

We hypothesize that the unidirectional alignment of cells is enforced by elastic interactions with the matrix, which favor the orientation of the rod-shaped objects (described by $\hat{m}$, Fig. 4) along the far-field director $\hat{n}_0$. To see this, we model the rod-shaped *P. aeruginosa* as spherocylinders (cylinders capped by two hemispheres at the ends) with tangential surface anchoring of $\hat{n}$ at the rod's surface (determined by polarizing microscopy). We consider the rod orientations in the matrix of liquid crystalline DNA ranging from parallel to perpendicular with respect to the LC director [Figs. 4(a)–4(c)]. For the tangential surface anchoring [12,27,28], computer-simulated director fields around the rod-shaped particles aligned parallel and/or perpendicular to $\hat{n}_0$ are shown in Figs. 4(d) and 4(e). Rods oriented along the far-field director $\hat{n}_0$ distort $\hat{n}$ and DNA orientations only at the rod's edges; the local LC director is parallel to the rod $\hat{n}\|\hat{m}$ along its length and is distorted only nearby the two semispheres capping the cylinder. $\hat{n}$ forms two boojums (surface point defects) at the two opposite rod's ends, Fig. 4(d). In contrast, elastic distortions persist along the entire rod's length if $\hat{m}\perp\hat{n}_0$ with one possible director structures containing two surface disclinations at the opposite sides along the rod, Fig. 4(e). Clearly, cell orientation perpendicular to $\hat{n}_0$ is much more costly in terms of the elastic free energy as compared to the parallel orientation.

To get quantitative insights into the physics behind alignment of bacteria in the DNA matrix (Fig. 1), we adopt the approach of Brochard and de Gennes [27,28] that was experimentally tested for nanowires in a thermotropic nematic [12]. In the limit of one-elastic-constant approximation $K=K_{11}=K_{22}=K_{33}$ (K_{11}, K_{22}, and K_{33} are Frank elastic constants for splay, twist, and bend, respectively) and when the ratio of rod's length L to its radius R is not very large, the elastic energy cost of realignment [27,28] for angle θ can be estimated as $U_{\text{elastic}}\approx 2\pi K\theta^2 L/\ln(2L/R)$. For typical $K\sim 10$ pN and size of the rod-shaped cells, one finds that energy difference is much larger than the thermal energy even for small angles θ, $U_{\text{elastic}}\sim 10^{-16}\theta^2 J\gg K_B T$. Moreover, the elastic torque exerted on bacteria by the LC medium $\partial U_{\text{elastic}}/\partial\theta\propto 4\pi K\theta L/\ln(2L/R)\sim 10^5\theta$ pN·nm is more than an order of magnitude larger than that generated by bacteria (usually up to 10^3 pN·nm) [29]. Thus, the departures of cell orientations from $\hat{n}_0$ are hindered by the medium's elasticity so that θ is small (Fig. 1) and the motility of *P. aeruginosa* is strongly influenced by the anisotropic matrix.

Since bacteria induce LC elastic distortions in the DNA matrix, their aggregation can decrease these elastic distortions and minimize the elastic free energy [11–14]. Moreover, aggregation is also favored by depletion interactions [30,31]. Interestingly, we observe no aggregates of wild-type bacteria. This contrasts with the behavior of colloidal particles in thermotropic nematics, in which the elasticity-mediated forces drive self-organization into chains and many other structures [11–14]. We believe that bacterial motility (possibly, along with repulsive electrostatic interactions between cells) can overcome elasticity-mediated and depletion interactions between the bacteria. Maximum elasticity-mediated forces between aligned rods with finite surface anchoring and quadrupolar-type distortions of $\hat{n}$ can be estimated as $F_{\text{elastic}}\propto C(W^2R^2/K)(2R/d)^6$ [14], where W is the strength of surface anchoring at the cell-LC matrix interface, d is the distance between the edges of the cylinders and C is a coefficient of the order of unity. Even though the exact values of $W\sim 10^{-5}$ J/m^2 and $K\sim 10$ pN are not known, these estimates show that the elastic forces for the typical $R\sim 300$ nm of the cells are $\leqslant 1$ pN; similarly, relevant entropic (depletion) forces are expected to be <1 pN [30,31]. These attractive forces are comparable or smaller than the viscous drag forces at (30–50) μm/s speeds of bacteria in water (estimated using the Stokes formula for micron-sized objects) and smaller than forces that can be generated by the bacteria when swimming using flagella, usually up to 10 pN [29] (note that bacteria attached to a surface can generate forces ~ 100 pN via retraction of type IV pili [29]).

The behavior of wild-type *P. aeruginosa* PAO1 has been compared against that of two motility mutants, a flagellum-deficient *fliC* mutant [22] and a type IV pili deficient mutant *pilA* [20]. We found cell ordering along the LC director for all three strains, with aligned motion (in parallel and antiparallel directions along $\hat{n}$) for the wild-type cells and (flagella-competent) *pilA* strains, and a "static" nematic (with only thermal motion) for the *fliC* mutant strains (which tend to aggregate). It is particularly interesting that the type IV pili deficient *pilA* strain exhibits the order. Type IV pili have been implicated in specific binding to DNA in previous stud-

ies, which occurs preferentially to pyrimidine residues, although there is no evidence of sequence-specific binding [3,4]. However, the pili-DNA binding alone is often not sufficient to describe the experimental observations [32]. Our results indicate that specific binding to DNA by the type IV pili is not a necessary condition for the nematiclike ordering of *Pseudomonas* in the matrix. Likewise, that the flagella-deficient *fliC* mutant (which can be viewed as a Brownian particle similar to colloidal ellipsoids or rod-shaped viruses [33]) also exhibits alignment indicates that the self-propelled nature of bacteria does not impinge on the observed alignment but helps to overcome elasticity- and depletion-mediated cell aggregation. These results are consistent with the elastic origin of the bacterial ordering and indicate that elasticity-mediated forces between the DNA matrix and bacteria may play a role in cell-matrix interactions [2–4,32,34–38]. Moreover, since bacteria can move along directed linear trajectories in regions of local nematic matrix alignment, these results may have implications for regulation of bacterial movement within biofilms.

To conclude, we have demonstrated that elastic forces exerted by the LC matrix of concentrated DNA can be used to order rod-shaped bacteria and that behavior of planktonic bacteria is strongly modified by the extracellular polymeric matrices. Elasticity-mediated alignment has a potential to be used for alignment of other nonspherical active particles and for directed self-assembly of nanostructured metamaterials.

We acknowledge support of the Institute for Complex Adaptive Matter, the NSF Grants No. DMR-0804363, DMR-0645461, DMR-0820579, and No. CBET08-27293, Water CAMPWS, and the RPI-UIUC NSEC. Part of this work was performed at the Frederick Seitz Materials Research Lab.

[1] H. Lodish *et al.*, *Molecular Cell Biology*, 5th ed. (W. H. Freeman, New York, 2004).
[2] C. Fuqua, M. R. Parsek, and E. P. Greenberg, Annu. Rev. Genet. **35**, 439 (2001).
[3] C. B. Whitchurch, T. Tolker-Nielsen, P. C. Ragas, and J. S. Mattick, Science **295**, 1487 (2002).
[4] E. J. van Schaik *et al.*, J. Bacteriol. **187**, 1455 (2005).
[5] B. Perks and J. K. Shute, Am. J. Respir. Crit. Care Med. **162**, 1767 (2000).
[6] D. B. Weibel, W. R. DiLuzio, and G. M. Whitesides, Nat. Rev. Microbiol. **5**, 209 (2007).
[7] S. Takeuchi, W. R. DiLuzio, D. B. Weibel, and G. M. Whitesides, Nano Lett. **5**, 1819 (2005).
[8] L. Xu *et al.*, Nano Lett. **7**, 2068 (2007).
[9] S. Park *et al.*, Science **301**, 188 (2003).
[10] V. Berry, S. Rangaswamy, and R. F. Saraf, Nano Lett. **4**, 939 (2004).
[11] P. Poulin, H. Stark, T. C. Lubensky, and D. A. Weitz, Science **275**, 1770 (1997).
[12] C. Lapointe *et al.*, Science **303**, 652 (2004).
[13] J. C. Loudet, P. Barois, and P. Poulin, Nature (London) **407**, 611 (2000).
[14] I. I. Smalyukh, O. D. Lavrentovich, A. N. Kuzmin, A. V. Kachynski, and P. N. Prasad, Phys. Rev. Lett. **95**, 157801 (2005); I. I. Smalyukh, A. V. Kachynski, A. N. Kuzmin, and P. N. Prasad, Proc. Natl. Acad. Sci. U.S.A. **103**, 18048 (2006).
[15] D. T. Chen *et al.*, Phys. Rev. Lett. **99**, 148302 (2007).
[16] L. Onsager, Ann. N.Y. Acad. Sci. **51**, 627 (1949).
[17] R. A. Simha and S. Ramaswamy, Phys. Rev. Lett. **89**, 058101 (2002).
[18] S. K. Kim and D. Kaiser, Science **249**, 926 (1990).
[19] B. V. Jones, R. Young, E. Mahenthiralingam, and D. J. Stickler, Infect. Immun. **72**, 3941 (2004).
[20] J. D. Shrout *et al.*, Mol. Microbiol. **62**, 1264 (2006).
[21] A. Heydorn *et al.*, Appl. Environ. Microbiol. **68**, 2008 (2002).
[22] S. Chugani and E. Greenberg, Microb. Pathog **42**, 29 (2007).
[23] D. H. Bergey, J. G. Holt, N. R. Krieg, and P. H. A. Sneath, *Bergey's Manual of Determinative Bacteriology*, 9th ed. (Williams and Wilkins, Baltimore, 1994).
[24] I. I. Smalyukh, O. V. Zribi, J. C. Butler, O. D. Lavrentovich, and G. C. L. Wong, Phys. Rev. Lett. **96**, 177801 (2006).
[25] R. D. Deegan *et al.*, Nature (London) **389**, 827 (1997).
[26] P. M. Chaikin and T. C. Lubensky, *Principles of Condensed Matter Physics* (Cambridge University Press, Cambridge, 1995).
[27] F. Brochard and P.-G. de Gennes, J. Phys. (Paris) **31**, 691 (1970).
[28] C. J. Smith and C. Denniston, J. Appl. Phys. **101**, 014305 (2007).
[29] N. C. Darnton, L. Turner, S. Rojevsky, H. C. Berg, J. Bacteriol. **189**, 1756 (2007).
[30] R. Verma, J. C. Crocker, T. C. Lubensky, and A. G. Yodh, Phys. Rev. Lett. **81**, 4004 (1998).
[31] D. Kleshchanok, R. Tuinier, and P. R. Lang, J. Phys.: Condens. Matter **20**, 073101 (2008).
[32] S. S. Branda, A. Vik, L. Friedman, and R. Kolter, Trends Microbiol. **13**, 20 (2005).
[33] M. P. Lettinga, E. Barry, and Z. Dogic, Europhys. Lett. **71**, 692 (2005).
[34] M. Allesen-Holm *et al.*, Mol. Microbiol. **59**, 1114 (2006).
[35] M. Klausen *et al.*, Mol. Microbiol. **48**, 1511 (2003).
[36] E. J. van Schaik *et al.*, J. Bacteriol. **187**, 1455 (2005).
[37] F. C. Petersen, L. Tao, and A. A. Scheie, J. Bacteriol. **187**, 4392 (2005).
[38] K. D. Young, Microbiol. Mol. Biol. Rev. **70**, 660 (2006).